Siberian Branch of Russian Academy of Science
BUDKER INSTITUTE OF NUCLEAR PHYSICS

R.R.Akhmetshin, E.V.Anashkin, M.Arpagaus, V.M.Aulchenko,
V.S.Banzarov, L.M.Barkov, N.S.Bashtovoy, A.E.Bondar,
D.V.Bondarev, A.V.Bragin, D.V.Chernyak, A.S.Dvoretsky,
S.I.Eidelman, G.V.Fedotovich, N.I.Gabyshev, A.A.Grebeniuk,
D.N.Grigoriev, P.M.Ivanov, S.V.Karpov, V.F.Kazanin,
B.I.Khazin, I.A.Koop, P.P.Krokovny, L.M.Kurdadze,
A.S.Kuzmin, I.B.Logashenko, P.A.Lukin, A.P.Lysenko,
K.Yu.Mikhailov, I.N.Nesterenko, V.S.Okhapkin,
E.A.Perevedentsev, E.A.Panich, A.S.Popov, T.A.Purlatz,
N.I.Root, A.A.Ruban, N.M.Ryskulov, A.G.Shamov,
Yu.M.Shatunov, B.A.Shwartz, A.L.Sibidanov, V.A.Sidorov,
A.N.Skrinsky, V.P.Smakhtin, I.G.Snopkov, E.P.Solodov,
P.Yu.Stepanov, A.I.Sukhanov, V.M.Titov, J.A.Thompson,
Yu.V.Yudin, S.G.Zverev

STUDY OF THE ϕ DECAYS INTO $\pi^+\pi^-\gamma$, $\pi^0\pi^0\gamma$ AND $\eta\pi^0\gamma$ FINAL STATES

Budker INP 99-51

http://www.inp.nsk.su/publications

Novosibirsk
1999

STUDY OF THE ϕ DECAYS INTO $\pi^+\pi^-\gamma$, $\pi^0\pi^0\gamma$ AND $\eta\pi^0\gamma$ FINAL STATES

R.R.Akhmetshin, E.V.Anashkin, M.Arpagaus, V.M.Aulchenko, V.S.Banzarov, L.M.Barkov, N.S.Bashtovoy, A.E.Bondar, D.V.Bondarev, A.V.Bragin, D.V.Chernyak, A.S.Dvoretsky, S.I.Eidelman, G.V.Fedotovich, N.I.Gabyshev, A.A.Grebeniuk, D.N.Grigoriev, P.M.Ivanov, S.V.Karpov, V.F.Kazanin, B.I.Khazin, I.A.Koop, P.P.Krokovny, L.M.Kurdadze, A.S.Kuzmin, I.B.Logashenko, P.A.Lukin, A.P.Lysenko, K.Yu.Mikhailov, I.N.Nesterenko, V.S.Okhapkin, E.A.Perevedentsev, E.A.Panich, A.S.Popov, T.A.Purlatz, N.I.Root, A.A.Ruban, N.M.Ryskulov, A.G.Shamov, Yu.M.Shatunov, B.A.Shwartz, A.L.Sibidanov, V.A.Sidorov, A.N.Skrinsky, V.P.Smakhtin, I.G.Snopkov, E.P.Solodov, P.Yu.Stepanov, A.I.Sukhanov, V.M.Titov, Yu.V.Yudin, S.G.Zverev

Budker Institute of Nuclear Physics
630090 Novosibirsk, Russia

J.A.Thompson

University of Pittsburgh, Pittsburgh, PA 15260, USA

Abstract

Radiative decays of the ϕ meson have been studied using a data sample of about 20 million ϕ decays collected by the CMD-2 detector at VEPP-2M collider in Novosibirsk. From selected $e^+e^- \to \pi^0\pi^0\gamma$ and $e^+e^- \to \eta\pi^0\gamma$ events the following model independent results have been obtained:
$Br\phi \to \pi^0\pi^0\gamma) = (0.92 \pm 0.08 \pm 0.06) \times 10^{-4}$ for $M_{\pi^0\pi^0} > 700$ MeV,
$Br(\phi \to \eta\pi^0\gamma) = (0.90 \pm 0.24 \pm 0.10) \times 10^{-4}$.

It is shown that the intermediate mechanism $f_0(980)\gamma$ dominates in the $\phi \to \pi^+\pi^-\gamma$ and $\phi \to \pi^0\pi^0\gamma$ decays and the corresponding branching ratio is $Br(\phi \to f_0(980)\gamma) = (3.11 \pm 0.23) \times 10^{-4}$.

Selected $e^+e^- \to \mu^+\mu^-\gamma$ events were used to obtain
$Br(\phi \to \mu^+\mu^-\gamma) = (1.43 \pm 0.45 \pm 0.14) \times 10^{-5}$ for $E_\gamma > 20$ MeV.

Using the same data sample upper limits have been obtained for the C-violating decay of the ϕ:

$Br(\phi \to \rho\gamma) < 1.2 \times 10^{-5}$; and for the P- and CP-violating decays of the η at 90% CL:

$Br(\eta \to \pi^+\pi^-) < 3.3 \times 10^{-4}$,
$Br(\eta \to \pi^0\pi^0) < 4.3 \times 10^{-4}$.

Introduction

The electric dipole radiative decays of the ϕ meson are very interesting for the clarification of the nature of $f_0(980)$ and $a_0(980)$ mesons [1]. A search for these decays has been earlier performed by the ND group [2] and a number of new results has been recently published by SND [3,4] and CMD-2 [5,6] collaborations at the e^+e^- collider VEPP-2M [7] where the radiative decays $\phi \to \pi^0\pi^0\gamma$, $\phi \to \eta\pi^0\gamma$ and $\phi \to \pi^+\pi^-\gamma$ have been observed for the first time.

The mode with two charged pions has very large background because of the radiative processes $e^+e^- \to \pi^+\pi^-\gamma$ where a photon comes from initial electrons or from final pions. Therefore a signal from the $f_0(980)\gamma$ final state is seen as an interference structure at the energy $E_\gamma = \frac{m_\phi^2 - m_{f_0^2}}{2m_\phi} \approx 40$ MeV in the photon spectrum. The shape of this structure depends on the $f_0(980)$ mass and width. In our first paper [8] a search for the $\phi \to \pi^+\pi^-\gamma$ decay led to the upper limit of 3×10^{-5} that looked puzzlingly low compared to the decay $\phi \to \pi^0\pi^0\gamma$ observed with the branching ratio of about 1×10^{-4} [4]. As it was shown in [5,8,9], in case of the $f_0(980)\gamma$ mechanism it could be explained by the destructive interference between bremsstrahlung processes and the ϕ decay.

The purely neutral mode has no bremsstrahlung background and is the most efficient to study the $\phi \to f_0(980)\gamma$ decay and two pion mass spectrum. With the CMD-2 detector this mode as well as another ϕ decay with five photons in the final state $\phi \to \eta\pi^0\gamma$ have been studied and the first results [5] based on about 25% of the data confirmed those reported earlier by SND.

The CMD-2 detector described in detail elsewhere [10] has been taking data since 1992. In addition to the barrel CsI calorimeter, the endcap calorimeter made of BGO crystals was installed in 1995 making detector almost hermetic to the photons. The energy resolution for photons in the CsI calorimeter is about 8% independent of the energy and $\sigma_E/E = 4.6\%/\sqrt{E(GeV)}$ for the BGO calorimeter. The muon system uses streamer tubes grouped in two layers (inner and outer) with a 15 cm magnet yoke serving as an absorber and has 1-3 cm spatial resolution.

In this paper results of the study of the $\phi \to \pi^0\pi^0\gamma$, $\phi \to \pi^+\pi^-\gamma$ and $\phi \to \eta\pi^0\gamma$ are presented. In total the 14.2 pb^{-1} of data have been collected at 14 energy points around the ϕ mass and correspond to 20.6×10^6 of ϕ decays. For this analysis 13.1 and 12.8 pb^{-1} were used for the $\pi^+\pi^-\gamma$ and $\pi^0\pi^0\gamma$ decay modes respectively. Seven scans of this energy region were performed allowing to control systematic errors caused by the possible instability of detector systems. The results obtained from individual scans were found to be consistent.

$\pi^+\pi^-\gamma$ Channel

Selection of $\pi^+\pi^-\gamma$ Events

Event candidates were selected by requiring only two minimum ionizing tracks in DC and one or two photons with the energy greater than 20 MeV in the CsI calorimeter. The following selection criteria were used:

1. The average momentum of two charged particles is higher than 240 MeV/c to remove the background from $K_S \to \pi^+\pi^-$ decays.
2. Detected tracks have a polar angle between 1.05 and 2.1 radians so that they enter the inner muon system.
3. The sum of the energy depositions of two clusters associated with two tracks is less than 450 MeV to remove Bhabha events.
4. The radial distance of the closest approach of each track to the beam axis is less than 0.3 cm.
5. The Z-coordinate of the vertex (along the beam) is within 10 cm from the detector center. This cut reduces cosmic ray background by a factor of two.
6. Detected photons have a polar angle between 0.85 and 2.25 radians so that they enter the "good" region in the CsI barrel calorimeter. This requirement suppressed the background from the photons emitted by initial electrons.
7. Events with an invariant mass of two photons close to the π^0 mass $|m_{\gamma\gamma} - m_{\pi^0}| < 40$ MeV were removed.

After the above cuts the main background for the $\pi^+\pi^-\gamma$ final state comes from: a) the radiative process $e^+e^- \to \mu^+\mu^-\gamma$, b) the decay $\phi \to \pi^+\pi^-\pi^0$ when one of the photons from the π^0 escapes detection and c) collinear events $e^+e^- \to \mu^+\mu^-, \pi^+\pi^-$ in which secondary decays and interactions of muons or pions with the detector material produce a background cluster mimicking a photon.

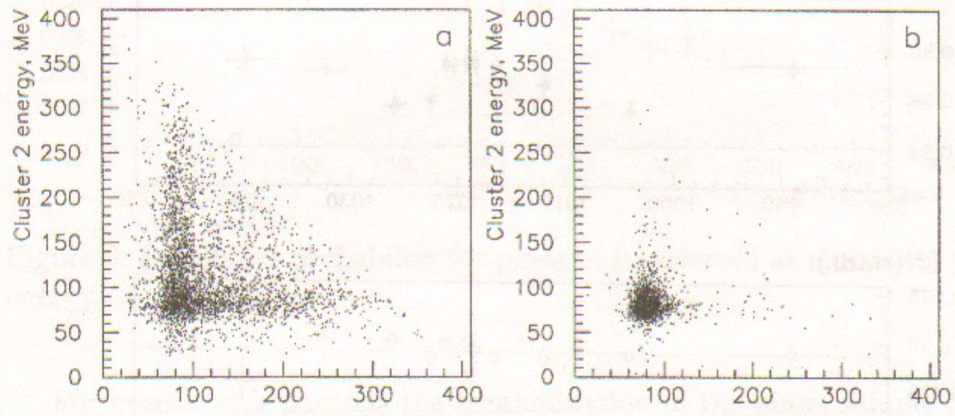

Figure 1: Calorimeter response for events with one or no hits in the muon system (a) and for events selected as muons (b).

Selection of $\mu^+\mu^-\gamma$ Events

The inner muon system was used to separate muons from pions. The requirement of hits in the inner muon system for both charged particles selects muon events, together with some pion events in which both pions pass the calorimeter without nuclear interaction.

Separation of pion and muon events in the CsI calorimeter is illustrated in Fig. 1, where scatter plots of the energy deposition of one track vs. that of the other one are presented for events with one or no hits in the muon system (a) and selected as muons (b). Energy depositions are corrected for the incident angle. Pions can have nuclear interactions and in some cases leave more energy, while muons mostly exhibit dE/dx losses only.

To select a cleaner sample of muon events, in addition to the information from the muon system both tracks were required to show only minimum ionizing energy deposition in the calorimeter (60-130 MeV). All the remaining events were considered as candidates to a pion sample. The pion sample

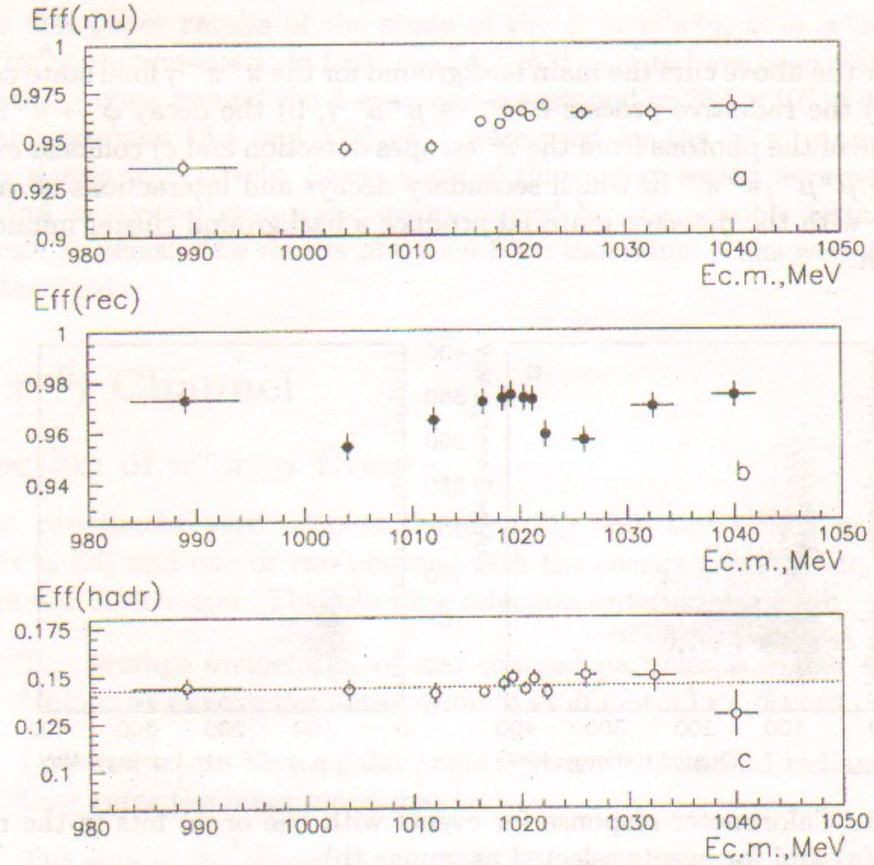

Figure 2: a.Muon system efficiency vs. energy. b.Reconstruction efficiency for DC. c.Probability for two pions to be selected as muons.

contains muons because of some inefficiency of the muon system while the muon sample contains pions since a pion can reach the muon system without nuclear interaction. The magnitudes of contamination were determined by studying correlations between the energy deposition in the CsI calorimeter and response of the muon system to collinear $\pi^+\pi^-$ and $\mu^+\mu^-$ events. The results of this study are shown in Fig. 2 for one of the experimental scans.

Figure 2a presents the muon system efficiency for different energy points. Only statistical errors are shown. The obtained number of pions and muons was corrected for the DC reconstruction efficiency shown in Fig. 2b. This efficiency was determined from collinear Bhabha events as described in [6]. The probability for two pions to be selected as muons is presented in Fig. 2c and is independent of the possible instability of the detection system. The overall systematic error in $\pi - \mu$ separation is estimated to be about 3% and

results in a correlated uncertainty in the selected number of pions and muons.

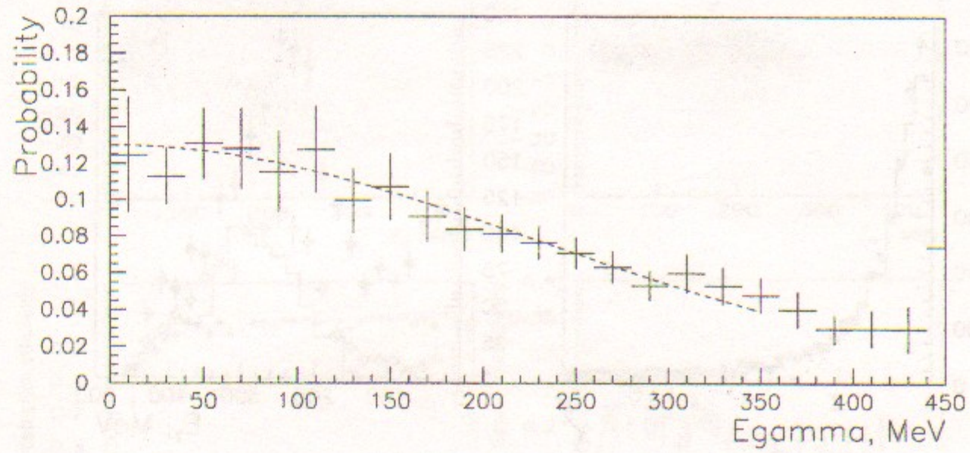

Figure 3: Simulated probability for pions to be selected as muons vs. photon energy.

For events with photons the contamination of the muon sample by pion events was studied using simulated $\pi^+\pi^-\gamma$ events. The probability of two pions to be selected as muons vs. photon energy is presented in Fig. 3 and was used for the correction of the photon spectrum. At a low photon energy this probability is consistent with that obtained from collinear events (see Fig. 2c).

Constrained Fit

To reduce the background from collinear events as well as that from the three pion annihilation a constrained fit was used requiring total energy-momentum conservation for a three body decay. About 20% of the selected events had an additional photon. In this case the constrained fit was applied to both possible combinations and that with a minimum χ^2 was chosen.

An additional cut was applied to the photon direction: an azimuthal angle should be more than 0.25 radians from the charged track direction. This cut removed the remaining collinear events with a background photon which survived after the constrained fit.

The χ^2/d.f. distribution for events selected as muons had very small background and was found to be in good agreement with simulation as shown in Fig. 4a. According to simulation a cut on the χ^2/d.f. to be less than 3

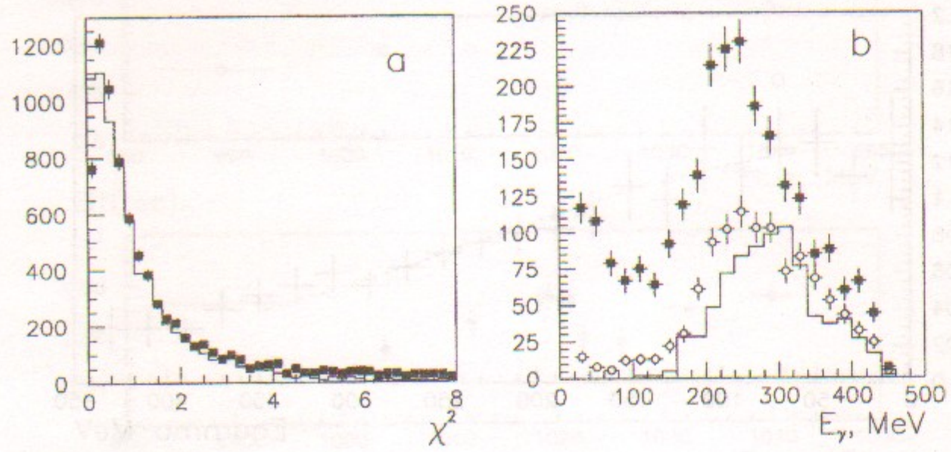

Figure 4: a. The χ^2/d.f. distribution for events selected as muons. The histogram is simulation. b. Photon spectrum for events selected as pions for χ^2/d.f.<3 (dark poins) and for $3 < \chi^2$/d.f. < 6 (open points). The histogram is simulation of background from $\pi^+\pi^-\pi^0$ events.

was imposed for pion and muon events selecting 95% of signal events.

After the above cut the pion sample still contained some background mainly from three pion decays. Such three pion background appears when one of the photons from the π^0 has the energy below 20 MeV and is not detected so that the event looks like a three body decay with the remaining photon energy higher than 150 MeV. The χ^2/d.f distribution for these events was flat and events with $3 < \chi^2$/d.f. < 6 were used to obtain the background spectrum shown in Fig. 4b by open marks. At each energy point the background spectrum was subtracted from one for the signal events.

As a result of the constrained fit one can obtain an improved estimate for the photon energy. This was studied by simulation and results are presented in Fig. 5. Simulation shows that after the constrained fit photons have energy resolution about 5 MeV in the whole energy range instead of $\sigma_{E_\gamma} = 8\% \times E_\gamma$ CsI resolution as shown in Figs. 5a,b. Figure 5c demonstrates the simulated photon detection efficiency in the CsI calorimeter vs. photon energy. The overall detector efficiency vs. photon energy for charged particles and photons is shown in Fig. 5d for $\pi^+\pi^-\gamma$ events.

Photons are required to be in the angular range 0.85-2.25 radians.

To extract the resonant contribution associated with the ϕ, two data sets

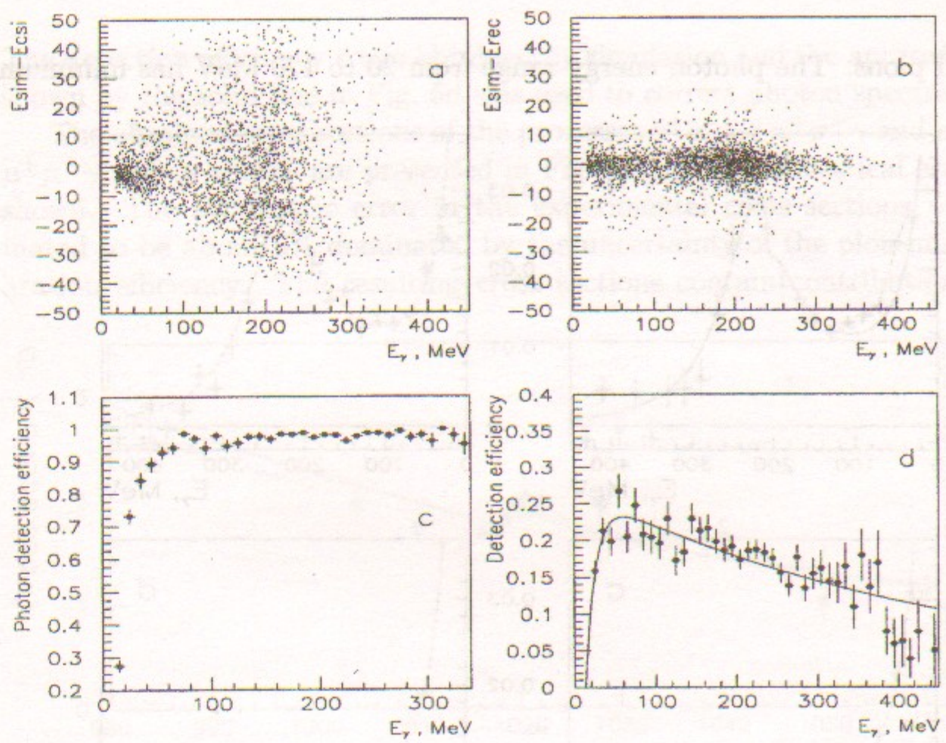

Figure 5: Study of simulated $\pi^+\pi^-\gamma$ events. a. Difference between the photon energy measured in the calorimeter and the initially simulated one vs. photon energy. b. Difference between the kinematically reconstructed photon energy and the initially simulated one vs. photon energy. c. Simulated photon detection efficiency in the CsI calorimeter. d. Overall detector efficiency vs. photon energy.

were used. Data collected at the energy points with $E_{c.m.}$ from 1016.0 to 1023.2 MeV with the integrated luminosity of 9.24 pb^{-1} were used for the "ϕ" region while those taken at $E_{c.m.}$ = 996-1013 and 1026-1060 MeV with the integrated luminosity of 3.89 pb^{-1} containing less than 3% of the ϕ decays were used for a background estimate ("off-ϕ" region).

Figures 6 present photon spectra obtained after background subtraction and corrections for the detector efficiency at the "ϕ" (a,c) and "off-ϕ" (b,d) regions for pions and muons respectively. The solid line presents theoretical calculations [9] taking into account the integrated luminosity at each energy point and $\rho - \omega$ mixing for the bremsstrahlung process. A peak at 220 MeV corresponds to the radiative process $e^+e^- \to \rho\gamma$ with the ρ decay into two

charged pions. The photon energy range from 20 to 120 MeV has minimum

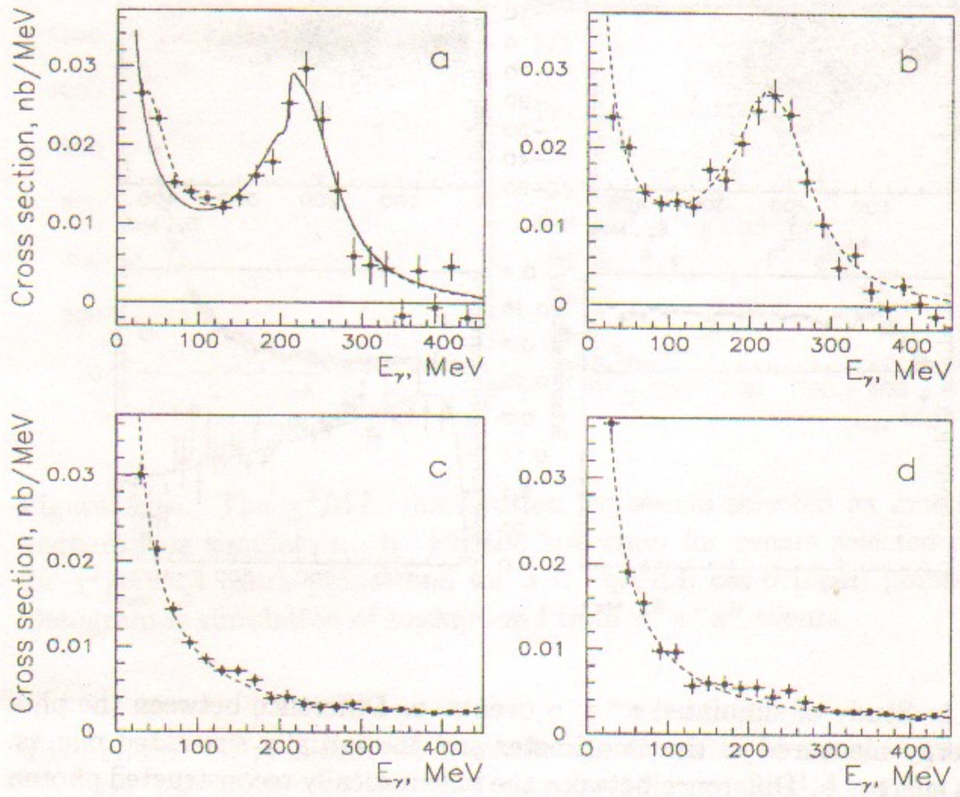

Figure 6: a. Photon spectrum for $\pi^+\pi^-\gamma$ events at the "ϕ" region; Solid line is pure bremsstrahlung. Dashed line includes a possible f_0 signal according to [9]. b. Photon spectrum for $\pi^+\pi^-\gamma$ events at the "off-ϕ" region; c,d. The same spectra for $\mu^+\mu^-\gamma$ events.

background and some excess of events over the expected bremsstrahlung spectrum can be seen in the $\pi^+\pi^-\gamma$ sample at the "ϕ" region (the dashed line in Fig. 6a). In total, 30175 $\pi^+\pi^-\gamma$ events and 27188 $\mu^+\mu^-\gamma$ events have been selected in this energy range.

Cross Section Study

The cross section for each energy point was calculated as $\sigma = N_{ev}/(\mathrm{L}\cdot\epsilon)$. N_{ev} is the number of selected events with photons in the energy range from 20 to 120 MeV. The integrated luminosity L for each energy point was determined from Bhabha events with about 2% systematic accuracy [6].

The detection efficiency ϵ was obtained by simulation and the approximation shown by the solid line in Fig. 5d was used to correct photon spectra.

The obtained cross sections of the processes $e^+e^- \to \pi^+\pi^-\gamma$ and $e^+e^- \to \mu^+\mu^-\gamma$ versus energy are presented in Fig. 7a,b. Only statistical errors are shown. The systematic error in the experimental cross sections was estimated to be about 5% dominated by the uncertainty of the pion-muon separation efficiency. The resulting cross sections contain contributions from

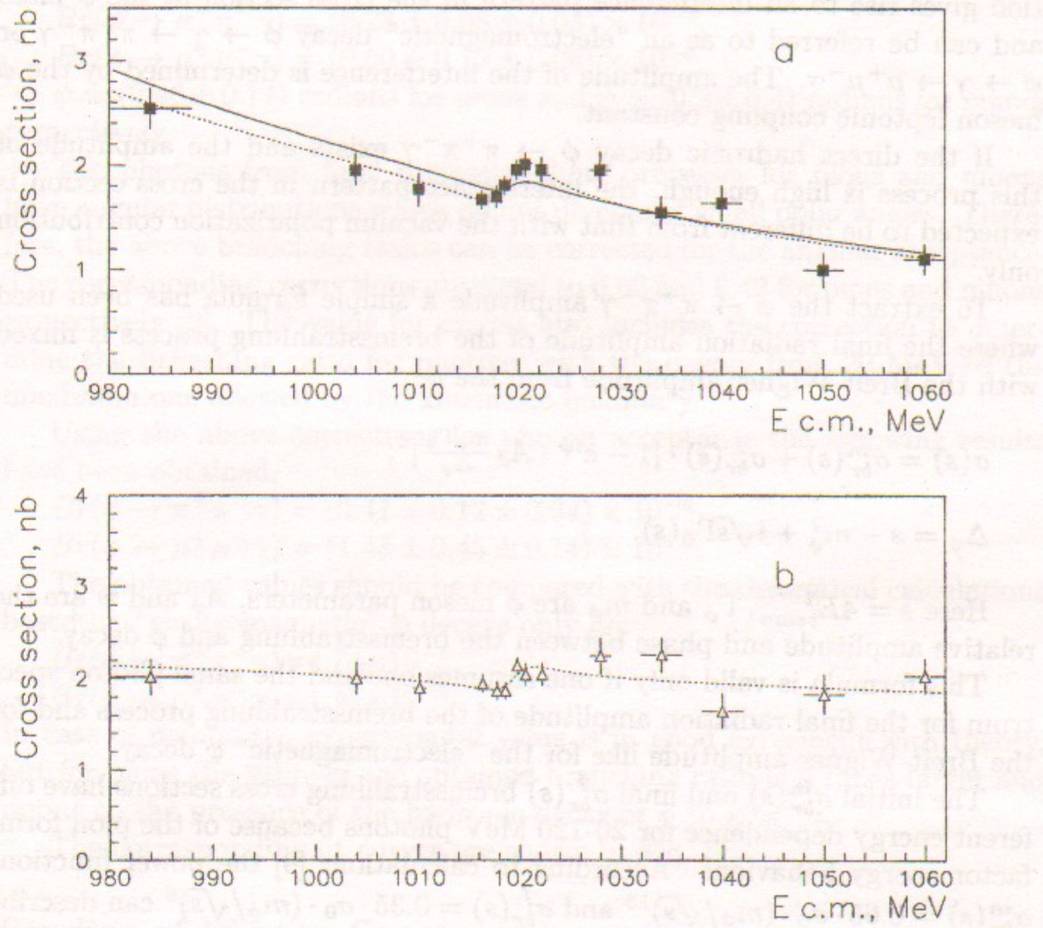

Figure 7: a. Cross section for $e^+e^- \to \pi^+\pi^-\gamma$. Lines are theoretical predictions in case of no direct ϕ decay (solid line) and best fit (dotted line). b. Cross section for $e^+e^- \to \mu^+\mu^-\gamma$ with the theoretical prediction.

bremsstrahlung by initial and final particles as well as the possible direct hadronic decay $\phi \to \pi^+\pi^-\gamma$.

The bremsstrahlung process from initial particles is suppressed by selecting photons transverse to the beam direction, but it still accounts for about 2/3 [9] of the observed $e^+e^- \to \pi^+\pi^-\gamma$ and one half of the $e^+e^- \to \mu^+\mu^-\gamma$ cross section.

The bremsstrahlung process from the final particles includes the ϕ contribution to the photon propagator (vacuum polarization). This contribution gives rise to an interference pattern in the cross section at the ϕ mass and can be referred to as an "electromagnetic" decay $\phi \to \gamma \to \pi^+\pi^-\gamma$ or $\phi \to \gamma \to \mu^+\mu^-\gamma$. The amplitude of the interference is determined by the ϕ meson leptonic coupling constant.

If the direct hadronic decay $\phi \to \pi^+\pi^-\gamma$ exists and the amplitude of this process is high enough, the interference pattern in the cross section is expected to be different from that with the vacuum polarization contribution only.

To extract the $\phi \to \pi^+\pi^-\gamma$ amplitude a simple formula has been used where the final radiation amplitude of the bremsstrahlung process is mixed with the Breit-Wigner amplitude from the ϕ:

$$\sigma(s) = \sigma^{in}_{br}(s) + \sigma^{f}_{br}(s) \cdot |1 - e^{i\psi} \cdot A_\phi \frac{m_\phi \Gamma_\phi}{\Delta_\phi}|^2;$$

$$\Delta_\phi = s - m^2_\phi + i\sqrt{s}\Gamma_\phi(s).$$

Here $s = 4E^2_{beam}$, Γ_ϕ and m_ϕ are ϕ meson parameters, A_ϕ and ψ are the relative amplitude and phase between the bremsstrahlung and ϕ decay.

This formula is valid only if one assumes one and the same photon spectrum for the final radiation amplitude of the bremsstrahlung process and for the Breit-Wigner amplitude like for the "electromagnetic" ϕ decay.

The initial $\sigma^{in}_{br}(s)$ and final $\sigma^{f}_{br}(s)$ bremsstrahlung cross sections have different energy dependence for 20-120 MeV photons because of the pion formfactor energy behaviour. According to calculations [9] the power functions $\sigma^{in}_{br}(s) = 0.65 \cdot \sigma_0 \cdot (m_\phi/\sqrt{s})^{13}$ and $\sigma^{f}_{br}(s) = 0.35 \cdot \sigma_0 \cdot (m_\phi/\sqrt{s})^{9}$ can describe the bremsstrahlung process $e^+e^- \to \pi^+\pi^-\gamma$ in our energy range. The parameter σ_0 represents the total cross section at the ϕ mass. The function $\sigma^{in}_{br}(s) = \sigma^{f}_{br}(s) = 0.5 \cdot \sigma_0(m^2_\phi/s)$ was used for muons.

The fit of experimental data with σ_0, peak amplitude A_ϕ and ψ as free parameters shows good agreement of obtained cross sections with the theoretical calculations [9]:
$\sigma^{exp}_0/\sigma^{th}_0 = 1.02 \pm 0.02 \pm 0.03$,
$\sigma^{exp}_0/\sigma^{th}_0 = 0.97 \pm 0.02 \pm 0.03$

for pions and muons respectively. The above values indicate also that the $\mu - \pi$ separation uncertainty does not exceed the estimated systematic error.

Using the obtained amplitude one can calculate peak cross section $\sigma(\phi \to \pi\pi\gamma) = |A|^2 \cdot \sigma^{f}_{br}(m^2_\phi)$ and the decay branching ratio can be calculated as $Br(\phi \to \pi\pi\gamma) = \sigma(\phi \to \pi\pi\gamma)/\sigma^{\phi}_{tot}$, where σ^{ϕ}_{tot} is the total peak cross section of the ϕ resonance obtained from the leptonic width [11]. The following results have been obtained:

$Br(\phi \to \pi^+\pi^-\gamma) = (0.28 \pm 0.08 \pm 0.03) \times 10^{-4}$,
$Br(\phi \to \mu^+\mu^-\gamma) = (0.60 \pm 0.19 \pm 0.06) \times 10^{-5}$,
$\psi = (0.46 \pm 0.17)$ radians for pions and $\psi = (0.2 \pm 0.4)$ radians for muons respectively.

The photons from final bremsstruhlung processes for pions and muons have angular distributions which do not diverge at small polar angles. Therefore, the above branching ratios can be corrected for the angular acceptance. The corresponding corrections are equal to 0.68 and 0.42 for pions and muons respectively [9]. The value for muons also includes the correction to determine the branching ratio for photons with the energy from 20 MeV to the maximum one allowed by the kinematic boundary.

Using the above corrections for photon acceptance the following results have been obtained:

$Br(\phi \to \pi^+\pi^-\gamma) = (0.41 \pm 0.12 \pm 0.04) \times 10^{-4}$,
$Br(\phi \to \mu^+\mu^-\gamma) = (1.43 \pm 0.45 \pm 0.14) \times 10^{-5}$.

The obtained values should be compared with the theoretical calculations based on "electromagnetic" ϕ decays only [9]:

$Br(\phi \to \pi^+\pi^-\gamma) = 4.74 \times 10^{-6}$,
$Br(\phi \to \mu^+\mu^-\gamma) = 1.15 \times 10^{-5}$.

In case of muons the experimental value is in good agreement with theory, but for pions the value of the obtained branching ratio is 9 times larger and points to the presence of the hadronic decay of ϕ to $\pi^+\pi^-\gamma$.

The corresponding fit curves are shown in Fig. 7.

Studies of Photon Spectra

To search for the $\phi \to f_0(980)\gamma$ decay contribution to the observed $\phi \to \pi^+\pi^-\gamma$ decay, photon energy spectra were studied. The photon spectra from the "ϕ" region are shown in Fig. 8 for six c.m.energy points and photons in the 20-160 MeV energy range. The spectra were corrected for all experimental inefficiencies and normalized to the integrated luminosity.

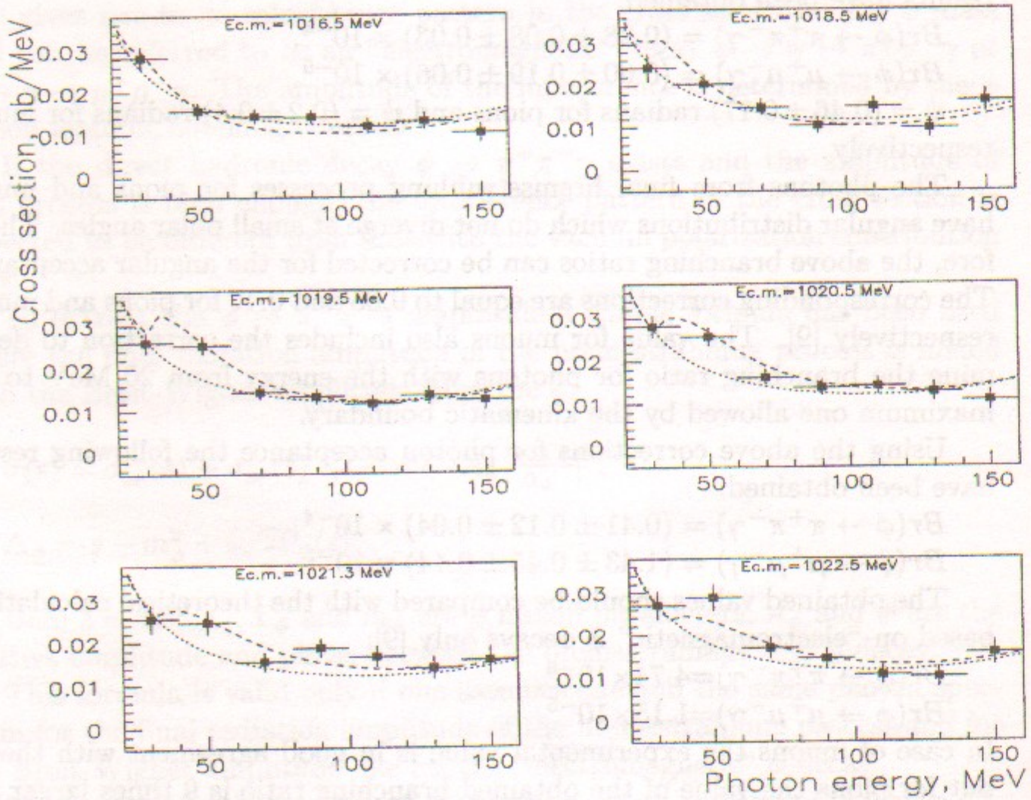

Figure 8: Photon spectra for six c.m.energy points in the "ϕ" region. Lines are theoretical predictions for the four quark model (dashed line) and pure bremsstrahlung spectra (dotted line).

The signal from the decay of the $\phi \to f_0(980)\gamma$ is seen as a structure in the photon spectra at 40-60 MeV. Also shown by the dotted lines are the theoretical predictions for the bremsstrahlung spectra [9,12] including vacuum polarization .

Because of the presence of the resonance in the photon spectra the branching ratio obtained in the previous chapter for the $\phi \to \pi^+\pi^-\gamma$ decay can be used only as some indication to the existence of the ϕ hadronic decay into this mode.

It should be mentioned that the excess of events over the bremsstrahlung spectra cannot be used for the branching ratio calculation. As it was shown in [5,8,9], the destructive interference with the bremsstrahlung process can reduce a visible signal in the selected energy range for photons (see discussion below).

$\phi \to \pi^0\pi^0\gamma$ channel

Selection of $\pi^0\pi^0\gamma$ Events

Events of this decay were selected from a sample of purely neutral events with the following criteria:

1. There are five or more photons in the CsI and BGO calorimeters with the total energy deposition $E_{tot} > 1.75 \cdot E_{beam}$. From the Monte Carlo simulation of the $\pi^0\pi^0\gamma$ events well reproducing the resolution over E_{tot} it follows that after this cut 97% of signal events remain. At least three photons are in the CsI calorimeter to have a high trigger efficiency [13].

2. All photons are in the polar angle 0.6-2.54 radians and have energy higher than 20 MeV.

3. To select $\pi^0\pi^0\gamma$ events the constrained fit with the requirement of energy-momentum conservation was performed in which two best combinations of photon pairs with π^0 masses were found. Events with $\chi^2 < 6$ were taken for further analysis. The χ^2 distribution after the constrained fit is shown in Fig. 9a. This cut suppresses to the 10^{-3} level the background from the $\phi \to K^0_S K^0_L$ decay mode when K^0_S decays to $\pi^0\pi^0$ and K^0_L produces the fifth cluster in the calorimeter.

4. Photons from reconstructed π^0's in the BGO calorimeter have energy higher than 40 MeV. This cut removed incorrectly reconstructed events with photons from the beam background.

5. A selection cut $|(P^1_{\pi^0} - P^2_{\pi^0})/(P^1_{\pi^0} + P^2_{\pi^0})| < 0.8$, where $P^1_{\pi^0}, P^2_{\pi^0}$ were pion momenta, was applied removing incorrect combinations when low energy free photon substituted one in the reconstructed π^0.

The χ^2 distribution after the constrained fit is shown in Fig. 9a.

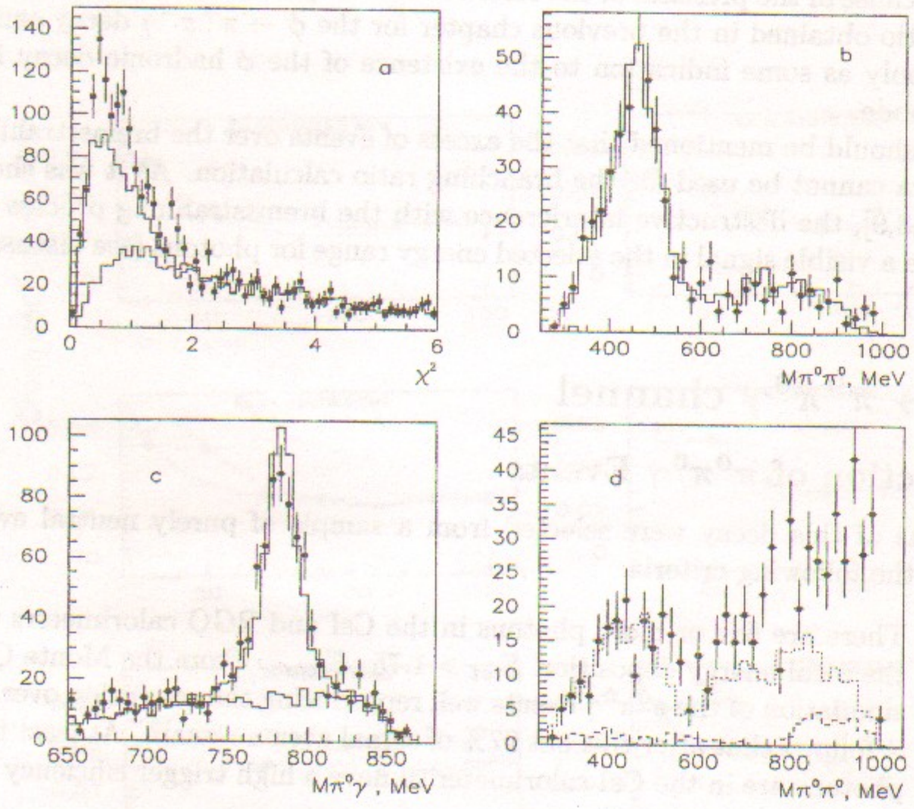

Figure 9: Study of the $\phi \to \pi^0\pi^0\gamma$ events: a. The χ^2 distribution for a five photon sample after the constrained fit. Histograms present the normalized simulated contribution from $\eta\gamma$ events (lower) and a sum of this distribution with that for $\omega\pi^0$ events (upper); b. The $\pi^0\pi^0$ invariant mass for events with $2.4 < \chi^2 < 6$. The histogram is simulation of $\eta\gamma$ events ; c. The $\pi^0\gamma$ invariant mass; d. The $\pi^0\pi^0$ invariant mass for events with $\chi^2 < 2.4$. Histograms show a contribution from $\omega\pi^0$ events after "anti-ω" cut (dashed) and a sum of this contribution with $\eta\gamma$ background (dotted).

Background Subtraction

The main background to events of interest comes from the processes $\phi \to \eta\gamma$, $\eta \to \pi^0\pi^0\pi^0$ with two lost photons and from $e^+e^- \to \omega\pi^0$ with the $\omega \to \pi^0\gamma$ decay.

The subtraction of the background from $\eta\gamma$ events was performed according to the simulation. The invariant mass of the $\pi^0\pi^0$ system for $2.4 < \chi^2 < 6$ is shown in Fig. 9b and demonstrates good agreement of the observed background spectrum with simulation. The normalization of observed background events to the collected integrated luminosity gives $N_\phi = (20.6 \pm 1.0)$ millions of ϕ decays in agreement with the (18.8 ± 0.9) millions obtained from the analysis of seven photon events from the $\phi \to \eta\gamma \to \pi^0\pi^0\pi^0\gamma$ decay [6]. The latter number was used for the normalization of signal events.

The invariant mass of $\pi^0\gamma$ for selected events is shown in Fig. 9c and demonstrates the presence of events from $e^+e^- \to \omega\pi^0$ process. The number of $\omega\pi^0$ events was found to be 506 ± 28 with the $\pi^0\gamma$ mass (782.0 ± 0.9) MeV close to the world average value [11]. These events were used to check the above cut efficiencies and event selection criteria. By looking for the $\omega\pi^0$ signal in a sample of six and seven photon events it was confirmed that 92% of signal events had exactly five photons. This was used for the efficiency correction. The simulated detection efficiency for $e^+e^- \to \omega\pi^0$ events was found to be $(14.4 \pm 0.1)\%$.

The cross section vs. energy for $e^+e^- \to \omega\pi^0 \to \pi^0\pi^0\gamma$ is presented in Fig. 10 and was fitted taking into account the interference of the non-resonant process with the ϕ decay. The values of the parameters of the $\phi \to \omega\pi^0$ decay were taken from [14]. The obtained non-resonant cross section at $2E_{beam} = m_\phi$ is $\sigma_0 = (0.58 \pm 0.02 \pm 0.04)$ nb and is consistent with that measured by SND [14]. The second error represents the systematic uncertainty caused by background subtraction.

The "anti-ω" cut $M_{inv}(\pi^0\gamma) < 750$ MeV reduces the admixture of $\omega\pi^0$ events to an about 5% level (see dashed histogram in Fig. 9d). However, it does not completely remove $\omega\pi^0$ events mostly because of some incorrectly reconstructed events when a free photon substitutes one in the reconstructed π^0. These incorrect combinations were studied using simulated $\omega\pi^0$ events and experimental events from the "off-ϕ" region where the process $e^+e^- \to \omega\pi^0$ dominates. The ratio of the number of incorrectly reconstructed events to the total number of $\omega\pi^0$ events was found to be 0.060 ± 0.003 for simulation and 0.09 ± 0.02 for experimental ones. The difference was used for a systematic error estimation in the above 5% admixture.

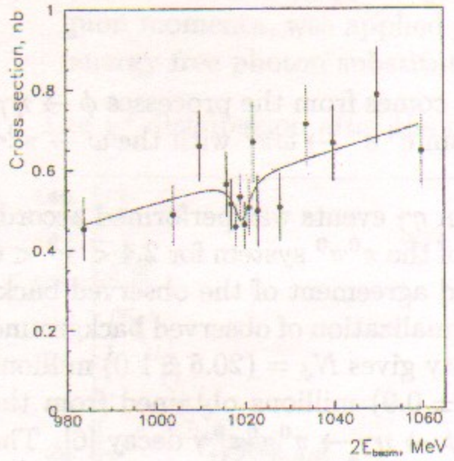

Figure 10: The cross section vs. energy for selected $\omega\pi^0$ events.

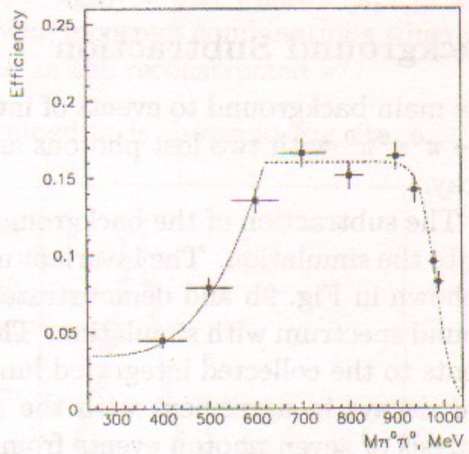

Figure 11: The simulated efficiency vs. $\pi^0\pi^0$ invariant mass. The line is an approximation used for calculations.

Branching Ratio Calculation

The invariant mass distribution of the $\pi^0\pi^0$ system for $\chi^2 < 2.4$ is shown in Fig. 9d with the expected backgrounds from $\omega\pi^0$ after the "anti-ω" cut and from $\eta\gamma$ events. The distribution demonstrates the increase of the number of events with a high invariant mass (a free photon of low energy). In total, 268 ± 27 of $\pi^0\pi^0\gamma$ events have been found after background subtraction.

The detection efficiency as a function of the $\pi^0\pi^0$ invariant mass was obtained using simulation of the process $e^+e^- \to X(M)\gamma$ where X(M) was a particle with a small width and variable mass M decaying into $\pi^0\pi^0$. The $dN/d\theta_\gamma \approx (1+cos^2(\theta_\gamma))$ angular distribution of the free photon was assumed. The obtained detection efficiency vs. the $\pi^0\pi^0$ invariant mass is presented in Fig. 11.

The $\pi^0\pi^0$ mass spectrum was obtained from the experimental distribution (Fig. 9d) after background subtraction and taking into account the detection efficiency for each histogram bin. The spectrum was normalized to the number of ϕ decays obtained from the $\phi \to \eta\gamma \to 3\pi^0\gamma$ analysis. The resulting differential cross section vs. invariant mass is presented in Fig. 12a showing a resonance increase at high masses. Figure 12b presents the angular distribution for free photons for signal events with $M_{\pi^0\pi^0} > 800$ MeV.

The line shows the distribution expected for a scalar intermediate resonance: $dN/d\theta_\gamma \approx (1+cos^2(\theta_\gamma))$. Points with open marks show the angular distribution of the subtracted background. The branching ratio was calculated from

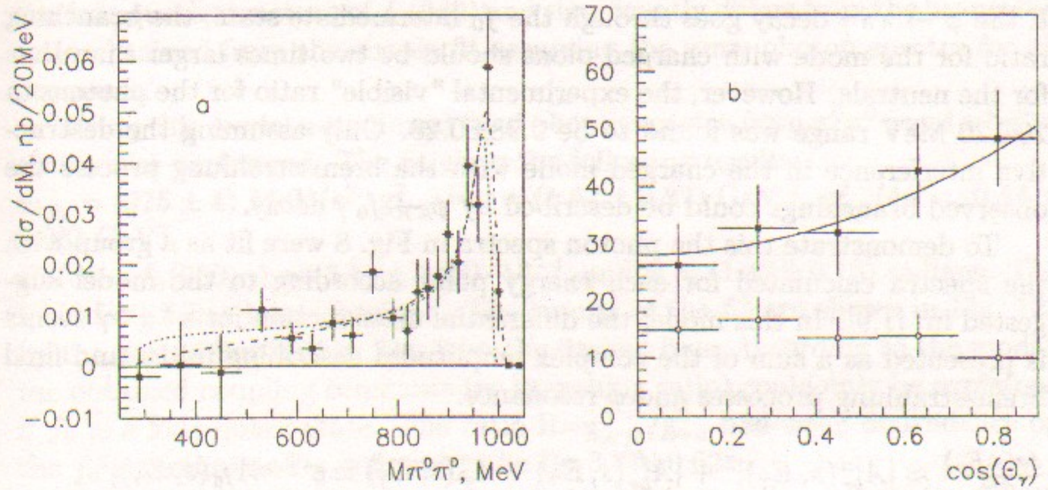

Figure 12: a. Differential cross section vs invariant mass. The dotted line is the four quark model fit with the 3.11×10^{-4} branching ratio. The dashed line is the narrow pole fit; b. Angular distribution for signal events and background (open marks). The line is $dN/d\theta_\gamma \approx (1 + cos^2(\theta_\gamma))$

the integral over the differential spectrum and was found to be

$Br(\phi \to \pi^0\pi^0\gamma) = (1.08 \pm 0.17 \pm 0.09) \times 10^{-4}$

for the whole invariant mass range. The systematic error comes from the uncertainty of the background subtraction (about 5%) and from the uncertainty of the number of ϕ mesons (about 5%). The main contribution to the statistical error comes from the region $M_{\pi^0\pi^0} < 550$ MeV because of the big uncertainty of the background subtraction.

This result can also be presented as:

$Br(\phi \to \pi^0\pi^0\gamma) = (1.06 \pm 0.09 \pm 0.06) \times 10^{-4}$ for $M_{\pi^0\pi^0} > 550$ MeV;

$Br(\phi \to \pi^0\pi^0\gamma) = (0.92 \pm 0.08 \pm 0.06) \times 10^{-4}$ for $M_{\pi^0\pi^0} > 700$ MeV;

$Br(\phi \to \pi^0\pi^0\gamma) = (0.57 \pm 0.06 \pm 0.04) \times 10^{-4}$ for $M_{\pi^0\pi^0} > 900$ MeV.

The results above are consistent with those presented by SND [14,4]. About a half of the signal has the free photon energy below 100 MeV.

It should be mentioned that only results for $M_{\pi^0\pi^0} > 700$ MeV can be considered as model independent. For lower masses the interference with $\omega\pi^0 \to \pi^0\pi^0\gamma$ nonresonant and with $\phi \to \rho\pi^0 \to \pi^0\pi^0\gamma$ resonant backgrounds can change the branching ratio. To extract these contributions a much better

measurement at lower masses is needed.

Data Interpretation

If the $\phi \to \pi\pi\gamma$ decay goes through the f_0 intermediate state, the branching ratio for the mode with charged pions should be two times larger than that for the neutrals. However, the experimental "visible" ratio for the photons in 20-120 MeV range was found to be 0.98±0.28. Only assuming the destructive interference in the charged mode with the bremsstrahlung process the observed branchings could be described by $\phi \to f_0\gamma$ decay.

To demonstrate this the photon spectra in Fig. 8 were fit as a group with the spectra calculated for each energy point according to the model suggested in [1,9]. In this model the differential cross section for $\pi^+\pi^-\gamma$ events is presented as a sum of the complex amplitudes describing initial and final bremsstrahlung processes and ϕ resonance:

$$\frac{d\sigma(s,E_\gamma)}{dE_\gamma} \approx |A^{in}_{br}(s,E_\gamma)|^2 + |A^{f}_{br}(s,E_\gamma) + A_\phi(s,E_\gamma) \pm e^{i\Psi}\cdot A_{f_0}(s,E_\gamma)|^2.$$

The amplitude $A_\phi(s,E_\gamma)$ introduces the influence of the ϕ upon the photon propagator (a vacuum polarization term). The amplitude $A_{f_0}(s,E_\gamma)$ represents the ϕ decay into the $\pi^+\pi^-\gamma$ final state via $f_0\gamma$. The model considers the f_0 meson as a two- or four-quark state or $K\bar{K}$ molecule depending on the values of the coupling constants $g^2_{K\bar{K}}/4\pi$ and $g^2_{\pi\pi}/4\pi$. Also included are the interference of ϕ amplitudes with the final bremsstrahlung process amplitude $A^f_{br}(s,E_\gamma)$ and correction for the $\pi^+\pi^-$ scattering at the final state [12] which gives with good accuracy an additional phase shift Ψ between the amplitudes of the ϕ and bremsstrahlung process. This shift was predicted to be 1.2-1.4 radians, but the sign of the term was unknown and was determined from the fit. All amplitudes have different dependence on s and E_γ.

Integration over E_γ from 20 to 120 MeV gives $\sigma(s)$ used for cross section aproximation in Fig. 7.

To fit the photon spectra in Fig. 8, the model parameters $g^2_{K\bar{K}}/4\pi$ and $g^2_{\pi\pi}/4\pi$ were varied to keep the $f_0(980)$ width at about 40 MeV [11]. The fit had the following free parameters: the branching ratio, $f_0(980)$ mass and phase shift Ψ. Only if the relative sign between f_0 amplitude and bremsstrahlung process in the charged mode was corresponding to destructive interference the data could be described by the model. The following results have been obtained:

$Br(\phi \to f_0(980)\gamma) = (1.93 \pm 0.46) \times 10^{-4}$;

$m_{f_0} = 976 \pm 5$ MeV;
$\Psi = 1.55 \pm 0.22$ radians.
The results above have weak dependence on the $f_0(980)$ width. The relatively large value of the branching ratio obtained in the fit is predicted only in case of the four quark structure of $f_0(980)$ and significantly differs from the branching ratio obtained from the simple fit assuming the same photon spectra for all processes.

Using this model a combined fit of photon spectra from $\pi^0\pi^0\gamma$ and $\pi^+\pi^-\gamma$ events was performed. The fit gives the following results:
$m_{f_0} = (975 \pm 4)$ MeV/c^2, $g^2_{K\bar{K}}/4\pi = (1.64 \pm 0.37)$ GeV ^{2}, $g^2_{\pi\pi}/4\pi = (0.44 \pm 0.06)$ GeV^2,
$Br(\phi \to f_0(980)\gamma) = (3.11 \pm 0.23)\cdot 10^{-4}$, and $\Psi = (1.42 \pm 0.18)$ radians. The χ^2/d.f.=1.5 has been obtained. The results of the fit are shown in Fig. 12a by the dotted line and in Fig. 8 by the dashed line. According to the model, the obtained coupling constants (or branching ratio) could only be explained if f_0 is a four quark state. The ratio R=$g^2_{K\bar{K}}/g^2_{\pi\pi}$ had weak dependence on the f_0 structure and was found to be R=3.77±0.62.

In the above interpretation the whole visible signal was associated with the $\phi \to f_0\gamma$ decay and the influence of other resonances $(\rho\pi, \sigma\gamma)$ was estimated [9,12] to be about 10-15%.

To understand how big the uncertainty of the branching ratio $\phi \to f_0\gamma$ can be, the narrow pole fit was performed. The $\pi^0\pi^0$ mass spectrum was fitted with the function:

$$\frac{d\sigma}{dM} \approx 2M\cdot(1-\frac{M^2}{4E^2_{beam}})\cdot\sqrt{1-\frac{4m^2_\pi}{M^2}}\cdot|\frac{m_{f(980)}\Gamma_{f(980)}}{\Delta_{f(980)}} + \frac{Ae^{i\psi}m_{f(1200)}\Gamma_{f(1200)}}{\Delta_{f(1200)}}|^2,$$

where $\Delta_f = M^2 - m^2_f + iM\Gamma(M)$. The parameters of the $f_0(1200)$ (or σ) resonance could not be extracted from our data and were fixed at $m_{f(1200)} = 1200$ MeV and $\Gamma_{f(1200)} = 600$ MeV. These parameters have very small influence on the result and instead of the $f_0(1200)$ Breit-Wigner the constant background amplitude $Ae^{i\psi}$ can be used. The relative phase ψ was found to be close to zero and fixed at that value.

The following parameters have been obtained:
$m_{f_0} = (987 \pm 7)$ MeV/c^2, $\Gamma_{f_0} = (56 \pm 20)$ MeV and the relative amplitude A=0.22±0.09 (or A=0.08±0.03 in case of constant background). The χ^2/d.f.=0.96 has been obtained. The result of the fit is shown in Fig. 12a by the dashed-dotted line.

The corresponding branching ratio (assuming that only 1/3 is seen in the $\pi^0\pi^0$ mode) $Br(\phi \to f_0(980)\gamma) = (1.5 \pm 0.5)\cdot 10^{-4}$ has been found.

The discussion above shows that obtained data cannot be interpreted without a resonance in the two pion mass spectrum at about 980 MeV both in charged and neutral modes and the $\phi \to f_0\gamma$ branching ratio cannot be lower than about $1.5 \cdot 10^{-4}$. As many authors agreed [15], the value that high cannot be explained in the frame of the two quark model of the $f_0(980)$ which normally predicted the branching ratio at the level of $0.5 \cdot 10^{-4}$. To study the influence of other resonances, better measurements of the $\pi\pi$ mass spectra are needed.

Search for $\phi \to \eta\pi^0\gamma$ Decay

Using the five photon final state, one can also look for the decay mode $\phi \to \eta\pi^0\gamma$ appearing when η decays into two photons. This analysis was based on the same event sample as in the study of the $\phi \to \pi^0\pi^0\gamma$ decay mode with the selection criteria described above.

The constrained fit finding one best combination of photon pairs with the π^0 mass and the pion momentum less than 350 MeV/c was performed. An additional requirement is that the difference in the energy of the photons from the found π^0 is less than 80%. It rejects background from low energy photons and increases the efficiency for events with a low energy free photon due to a smaller probability of wrong combinations.

The invariant masses of the remaining most energetic photon pairs are shown in Fig. 13a.

The cut $760 < M_{\pi^0\gamma} < 805$ MeV from the $\pi^0\pi^0\gamma$ reconstruction almost removes the background from $\omega\pi^0$. $\omega\pi^0$ events remaining after the "anti-ω" cut are shown by the dotted histogram.

At the broad background distribution the peak with 80 ± 22 events and $m_\eta = (545 \pm 4)$ MeV is seen. The solid histogram shows the sum of the simulated background from $\phi \to \eta\gamma \to 3\pi^0\gamma$ and remaining $\omega\pi^0$ events normalized to the number of ϕ decays. These simulated events were used for background subtraction. The dashed histogram at 550 MeV shows a simulated signal from the $\phi \to \eta\pi^0\gamma$ decay at 1×10^{-4} level.

The distributions over $cos\theta_\gamma$ and invariant mass $M_{\eta\pi^0}$ are shown in Figs. 13b,c for events with $510 < M_{\gamma\gamma} < 590$ MeV after background subtraction and taking into account the detection efficiency obtained by simulation (Fig. 13d). The following branching ratio

$Br(\phi \to \eta\pi^0\gamma) = (0.90 \pm 0.24 \pm 0.10) \times 10^{-4}$

has been obtained. The systematic error comes from the uncertainty of the background subtraction and of the number of ϕ's taken for normalization.

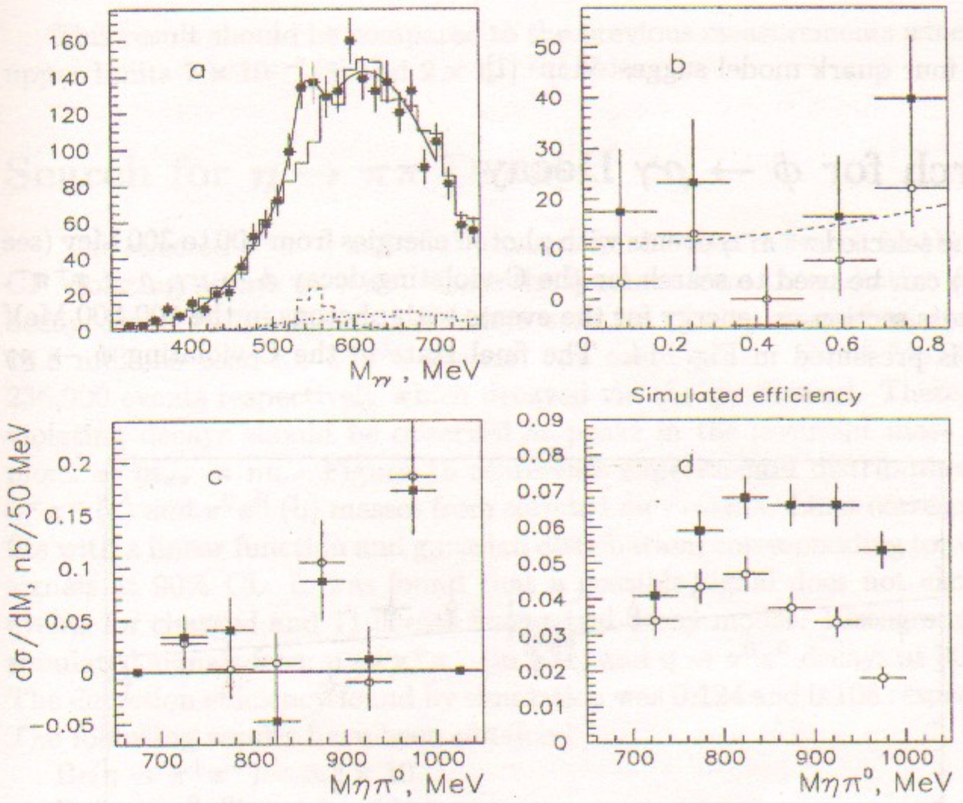

Figure 13: The $\phi \to \eta\pi^0\gamma$ study. Open marks are for "strong" cuts: a. Invariant masses of two photons with the highest energy for data (points) and simulation (histograms); b. $cos\theta_\gamma$ distribution for events around η mass after background subtraction. Line is expected $dN/d\theta_\gamma \approx (1 + cos^2(\theta_\gamma))$ distribution; c. The cross section vs. $\eta\pi^0$ mass distribution; d. The simulated detection efficiency vs. invariant mass.

To check the stability of the result these distributions were also obtained in the case of "strong" cuts when the additional requirement for the reconstructed photon with the highest energy was applied: $E_{\gamma max}/E_{beam} < 0.75$. This cut reduced the main background from $\phi \to \eta\gamma \to 3\pi^0\gamma$ by a factor of 4, but at the same time considerably reduced the detection efficiency at higher $\eta\pi^0$ invariant masses (opened marks in Fig. 13d). The number of observed signal events dropped to 37 ± 12 and the obtained branching ratio was the same within statistical errors.

The obtained invariant mass distribution shows the growth of the cross section to higher masses supporting the hypothesis about the $a_0(980)$ intermediate state. The obtained value of the branching ratio can be explained

in the four quark model suggested in [1].

Search for $\phi \to \rho\gamma$ Decay

The selected $\pi^+\pi^-\gamma$ events with photon energies from 100 to 300 Mev (see Fig. 6) can be used to search for the C-violating decay $\phi \to \rho\gamma$, $\rho \to \pi^+\pi^-$. The cross section vs. energy for the events with photons in the 100-300 MeV range is presented in Fig. 14. The final state in the C-violating $\phi \to \rho\gamma$

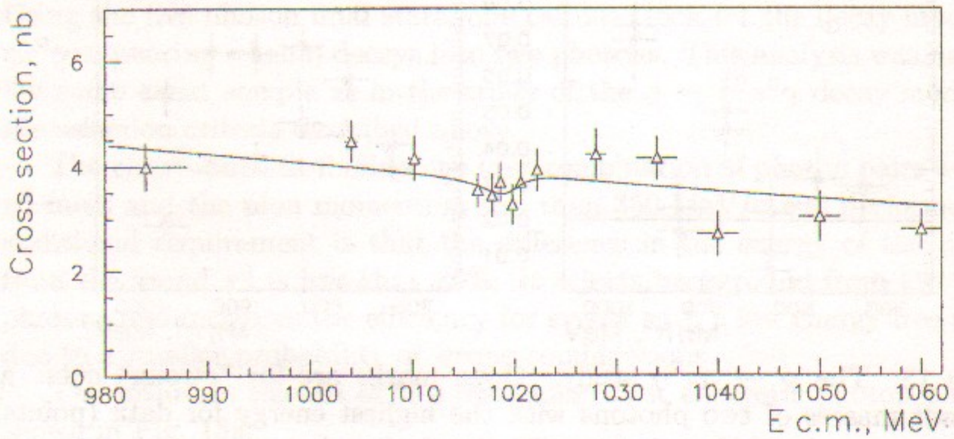

Figure 14: $\phi \to \rho\gamma$ search. The cross section for $\pi^+\pi^-\gamma$ events for photons in the 100-300 MeV region. The line is the best fit.

decay has the same quantum numbers as in the initial bremsstrahlung process which dominates in the cross section and to extract a possible signal the interference of these two processes is assumed:

$$\sigma(s) = \sigma_{br}^{in}(s) \cdot |1 - e^{i\psi} \cdot \sqrt{\frac{\sigma(\phi\to\rho\gamma)}{\sigma_{br}^{in}(s)}} \cdot \frac{m_\phi \Gamma_\phi}{\Delta_\phi}|^2,$$

where $\sigma_{br}^{in}(s) = \sigma_0(m_\phi^2/s)$. The comparison of the obtained cross section with the theoretical calculation [9] gives the ratio $\sigma_0^{exp}/\sigma_0^{th}$=1.04±0.03. As a result of the fit, $Br(\phi \to \rho\gamma) = \sigma(\phi \to \rho\gamma)/\sigma_{tot}^{\phi} = (0.3 \pm 0.5) \times 10^{-5}$ and $\psi = -0.9 \pm 1.0$ radians have been obtained. Taking into account the 80% detection efficiency, the corresponding upper limit is: $Br(\phi \to \rho\gamma) < 1.2 \times 10^{-5}$ at 90% C.L.

This result should be compared to the previous measurements which gave upper limits 7×10^{-4} [8] and 2×10^{-2} [16].

Search for $\eta \to \pi\pi$ Decays

The selected $\pi^+\pi^-\gamma$ and $\pi^0\pi^0\gamma$ events can be used to search for the P and CP violating decays $\eta \to \pi\pi$, where the η comes from the radiative $\phi \to \eta\gamma$ decay. From 19.7 millions of ϕ decays used for $\pi^+\pi^-\gamma$ channel analysis and 18.8 millions used for $\pi^0\pi^0\gamma$ channel one could expect about 248,000 and 236,000 events respectively which decayed via the $\eta\gamma$ channel. These P, CP violating decays should be observed as peaks in the invariant mass of two pions at $m_{\pi\pi} = m_\eta$. Figure 15 represents experimental distributions over $\pi^+\pi^-$ (a) and $\pi^0\pi^0$ (b) masses from selected $\pi\pi\gamma$ events. Lines correspond to fits with a linear function and gaussian distribution, corresponding to possible signals at 90% CL. It was found that a possible signal does not exceed 10 events for charged and 11 events for neutral decay modes. Histograms show simulated signals from $\eta \to \pi^+\pi^-$ (in box) and $\eta \to \pi^0\pi^0$ decays at 90% CL. The detection efficiency found by simulation was 0.124 and 0.108 respectively. The following results have been obtained:

$\mathrm{Br}(\eta \to \pi^+\pi^-) < 3.3 \times 10^{-4}$

$\mathrm{Br}(\eta \to \pi^0\pi^0) < 4.3 \times 10^{-4}$,

which should be compared to the best previous measurements 9×10^{-4} for the charged mode [8] and 7×10^{-4} for the neutral mode [18].

Conclusions

Using about 13 pb^{-1} of data collected around the ϕ meson (about 20 millions of the ϕ decays) $e^+e^- \to \pi^+\pi^-\gamma$ and $e^+e^- \to \mu^+\mu^-\gamma$ events were selected. For the first time the decay $\phi \to \pi^+\pi^-\gamma$ has been observed in the 20-120 MeV photon energy range and a fit assuming only contribution of the ϕ to the photon propagator gave the branching ratio:

$Br(\phi \to \pi^+\pi^-\gamma) = (0.41 \pm 0.12 \pm 0.04) \times 10^{-4}$.

This value is nine times higher than the expected and points to the presence of the hadronic decay of the ϕ into this final state. The analysis of the photon spectra shows the presence of a resonance with a mass of about 980 MeV and the obtained branching ratio can be affected by the complicated interference of hadronic ϕ decay with the bremsstrahlung process.

For muons the value

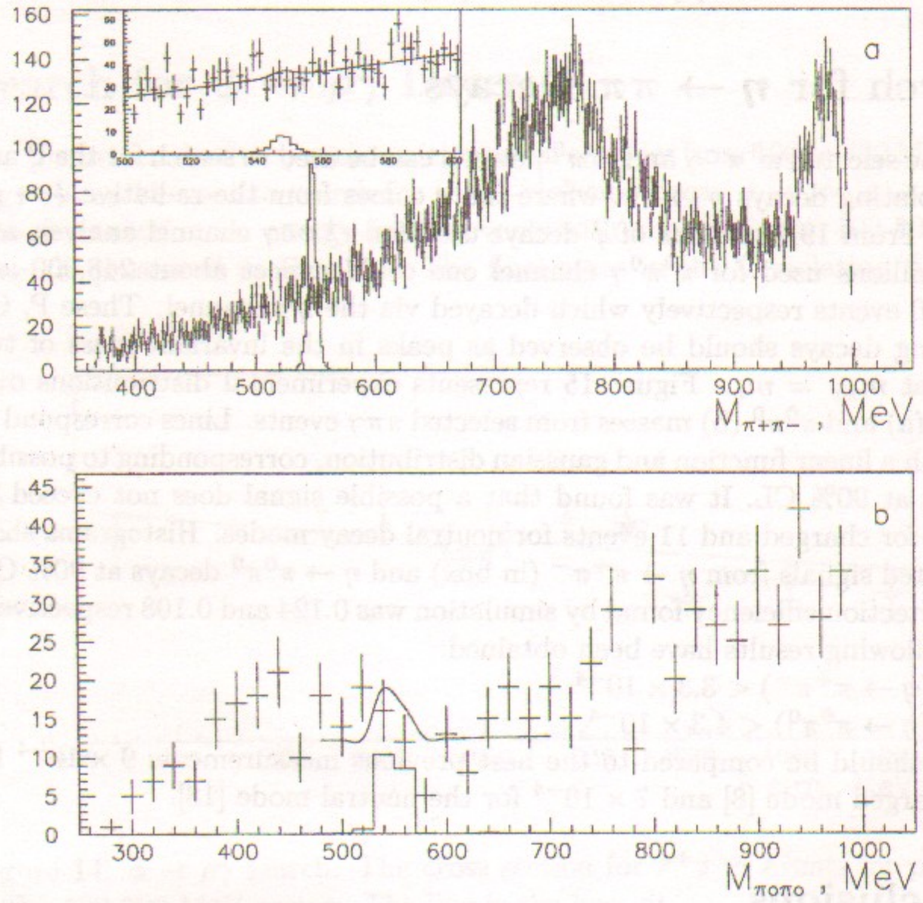

Figure 15: Search for $\eta \to \pi^+\pi^-$ and $\eta \to \pi^0\pi^0$ decays. Histograms are simulation. Lines show a possible signal at 90% CL.

$Br(\phi \to \mu^+\mu^-\gamma) = (1.43 \pm 0.45 \pm 0.14) \times 10^{-5}$
has been obtained for the photon energies $E_\gamma > 20 MeV$ consistent with the theoretical expectations.

The analysis of events with five photons with the reconstruction of the $\pi^0\pi^0\gamma$ and $\eta\pi^0\gamma$ final states gives the following model independent results:
$Br(\phi \to \pi^0\pi^0\gamma) = (0.92 \pm 0.08 \pm 0.06) \times 10^{-4}$ for $M_{\pi^0\pi^0} > 700$ MeV,
$Br(\phi \to \eta\pi^0\gamma) = (0.90 \pm 0.24 \pm 0.10) \times 10^{-4}$,
in agreement with those previously reported by the SND group [4,3]. Also shown is the resonance at 980 MeV in the $\pi^0\pi^0$ mass spectrum.

For the $\pi^0\pi^0\gamma$ channel the branching ratio obtained by integration over

the whole mass spectrum was found to be
$Br(\phi \to \pi^0\pi^0\gamma) = (1.08 \pm 0.17 \pm 0.09) \times 10^{-4}$,
but this result can be affected by the possible interference with $\omega\pi^0 \to \pi^0\pi^0\gamma$ or $\rho\pi^0 \to \pi^0\pi^0\gamma$ final states at $M_{\pi^0\pi^0} < 700$ MeV.

In the $\pi\pi\gamma$ channel the $\phi \to f_0(980)\gamma$ mechanism dominates and the most complete description both for charged and neutral modes can be obtained in the four quark model with the branching ratio
$Br(\phi \to f_0(980)\gamma) = (3.11 \pm 0.23) \times 10^{-4}$.
This result is model dependent and the presence of other resonances can decrease the branching ratio to about 1.5×10^{-4} which is still higher than the prediction of the two quark model [1,15]. The relatively low signal in the charged mode is explained by the destructive interference with the bremsstrahlung background. The discussed models give the following $f_0(980)$ parameters:
$m_{f_0} = (978 \pm 4 \pm 6)$ MeV, $W_{f_0} = (56 \pm 20 \pm 10)$ MeV,
where the second error represents a model dependent uncertainty.

In the $\eta\pi^0\gamma$ final state events with the high $\eta\pi^0$ invariant mass dominate. This supports the hypothesis about the $a_0(980)$ intermediate state. The obtained branching ratio is also higher than the prediction of the two quark model.

For the C violating decay of $\phi \to \rho\gamma$ and P,CP violating decays of $\eta \to \pi^+\pi^-$ and $\eta \to \pi^0\pi^0$ the following upper limits at 90% CL have been obtained:
$Br(\phi \to \rho\gamma) < 1.2 \times 10^{-5}$,
$Br(\eta \to \pi^+\pi^-) < 3.3 \times 10^{-4}$,
$Br(\eta \to \pi^0\pi^0) < 4.3 \times 10^{-4}$.
These results are the most stringent upper limits at the moment [11].

Acknowledgements

The authors are grateful to N.N.Achasov, V.V.Gubin, V.N.Ivanchenko, V.P.Druzhinin and A.I.Milstein for useful discussions and help with the data interpretation.

REFERENCES

1. N.N.Achasov and V.N.Ivanchenko, Nucl. Phys. **B315** (1989) 465.
2. S.I.Dolinsky *et al.*, Phys. Rep. **202** (1991) 99.
3. M.N.Achasov *et al.*, Phys. Lett. **B438** (1998) 441.

4. M.N.Achasov *et al.*, Phys. Lett. **B440** (1998) 442.
5. E.Solodov (CMD-2 collaboration), Proc. of the 29th Conf. on High Energy Phys. 19-24 July.1998, Vancouver, Canada.
6. R.R.Akhmetshin *et al.*, Preprint BudkerINP 99-11, Novosibirsk, 1999.
7. V.V.Anashin *et al.*, Preprint INP 84-114, Novosibirsk, 1984.
8. R.R. Akhmetshin *et al.*, Phys. Lett. **B415** (1997) 452.
9. N.N.Achasov, V.V.Gubin and E.P.Solodov, Phys. Rev. **D55** (1997) 2672.
10. G.A.Aksenov *et al.*, Preprint BudkerINP 85-118, Novosibirsk, 1985.
    E.V. Anashkin *et al.*, ICFA Instrumentation Bulletin **5** (1988) 18.
11. C.Caso *et al.*, Eur.Phys.J. **C3** (1998) 1, Review of Particle Physics.
12. N.N.Achasov and V.Gubin, Phys. Rev. **D57** (1998) 1987.
13. V.M.Aulchenko *et al.*, Preprint BudkerINP 92-28, Novosibirsk, 1992.
14. M.N.Achasov *et al.*, Phys. Lett. **B449** (1999) 122.
    Preprint BudkerINP 98-65, Novosibirsk, 1998.
15. S.Nussinov and Tran N. Truong, Phys. Rev. Lett. **63** (1989) 1349; A.A. Pivovarov, Soviet Physics - Lebedev Institute Reports **9** (1990) 12; N. Paver, contribution to the ϕ Factory Workshop at UCLA, April, 1990.; J.L. Lucio and J.Pestieau, Phys. Rev. **D42** (1990) 3253; S. Fajfer and R.J. Oakes, Phys. Rev. **D42** (1990) 2392. F.E. Close, N. Isgur and S. Kumano, Nucl. Phys. **B389** (1993) 513.
16. J.S.Lindsey *et al.*, Phys. Rev. **147** (1966) 913.
17. J.J.Thaler *et al.*, Phys. Rev. **D7** (1973) 2569.
18. M.N.Achasov *et al.*, Phys. Lett. **B425** (1998) 388.

R.R.Akhmetshin, E.V.Anashkin, M.Arpagaus, V.M.Aulchenko, V.S.Banzarov, L.M.Barkov, N.S.Bashtovoy, A.E.Bondar, D.V.Bondarev, A.V.Bragin, D.V.Chernyak, A.S.Dvoretsky, S.I.Eidelman, G.V.Fedotovich, N.I.Gabyshev, A.A.Grebeniuk, D.N.Grigoriev, P.M.Ivanov, S.V.Karpov, V.F.Kazanin, B.I.Khazin, I.A.Koop, P.P.Krokovny, L.M.Kurdadze, A.S.Kuzmin, I.B.Logashenko, P.A.Lukin, A.P.Lysenko, K.Yu.Mikhailov, I.N.Nesterenko, V.S.Okhapkin, E.A.Perevedentsev, E.A.Panich, A.S.Popov, T.A.Purlatz, N.I.Root, A.A.Ruban, N.M.Ryskulov, A.G.Shamov, Yu.M.Shatunov, B.A.Shwartz, A.L.Sibidanov, V.A.Sidorov, A.N.Skrinsky, V.P.Smakhtin, I.G.Snopkov, E.P.Solodov, P.Yu.Stepanov, A.I.Sukhanov, V.M.Titov, Yu.V.Yudin, S.G.Zverev

Study of the ϕ decays into $\pi^+\pi^-\gamma$, $\pi^0\pi^0\gamma$ and $\eta\pi^0\gamma$ final states

П.П. Ахметшин, Е.В. Анашкин и др. (всего 53 авторов)

Изучение распадов ϕ мезона в $\pi^+\pi^-\gamma$, $\pi^0\pi^0\gamma$ и $\eta\pi^0\gamma$ конечные состояния

Budker INP 99-51

Ответственный за выпуск А.М. Кудрявцев
Работа поступила 8.06.1999 г.

Сдано в набор 15.06.1999 г.
Подписано в печать 15.06.1999 г.
Формат бумаги 60×90 1/16 Объем 1.9 печ.л., 1.6 уч.-изд.л.
Тираж 150 экз. Бесплатно. Заказ N° 51

Обработано на IBM PC и отпечатано на
ротапринте ИЯФ им. Г.И. Будкера СО РАН
Новосибирск, 630090, пр. академика Лаврентьева, 11.

4. M.N.Achasov *et al.*, Phys. Lett. **B440** (1998) 442.
5. E.Solodov (CMD-2 collaboration), Proc. of the 29th Conf. on High Energy Phys. 19-24 July.1998, Vancouver, Canada.
6. R.R.Akhmetshin *et al.*, Preprint BudkerINP 99-11, Novosibirsk, 1999.
7. V.V.Anashin *et al.*, Preprint INP 84-114, Novosibirsk, 1984.
8. R.R. Akhmetshin *et al.*, Phys. Lett. **B415** (1997) 452.
9. N.N.Achasov, V.V.Gubin and E.P.Solodov, Phys. Rev. **D55** (1997) 2672.
10. G.A.Aksenov *et al.*, Preprint BudkerINP 85-118, Novosibirsk, 1985.
    E.V. Anashkin *et al.*, ICFA Instrumentation Bulletin **5** (1988) 18.
11. C.Caso *et al.*, Eur.Phys.J. **C3** (1998) 1, Review of Particle Physics.
12. N.N.Achasov and V.Gubin, Phys. Rev. **D57** (1998) 1987.
13. V.M.Aulchenko *et al.*, Preprint BudkerINP 92-28, Novosibirsk, 1992.
14. M.N.Achasov *et al.*, Phys. Lett. **B449** (1999) 122.
    Preprint BudkerINP 98-65, Novosibirsk, 1998.
15. S.Nussinov and Tran N. Truong, Phys. Rev. Lett. **63** (1989) 1349; A.A. Pivovarov, Soviet Physics - Lebedev Institute Reports **9** (1990) 12; N. Paver, contribution to the ϕ Factory Workshop at UCLA, April, 1990.; J.L. Lucio and J.Pestieau, Phys. Rev. **D42** (1990) 3253; S. Fajfer and R.J. Oakes, Phys. Rev. **D42** (1990) 2392. F.E. Close, N. Isgur and S. Kumano, Nucl. Phys. **B389** (1993) 513.
16. J.S.Lindsey *et al.*, Phys. Rev. **147** (1966) 913.
17. J.J.Thaler *et al.*, Phys. Rev. **D7** (1973) 2569.
18. M.N.Achasov *et al.*, Phys. Lett. **B425** (1998) 388.

R.R.Akhmetshin, E.V.Anashkin, M.Arpagaus, V.M.Aulchenko, V.S.Banzarov, L.M.Barkov, N.S.Bashtovoy, A.E.Bondar, D.V.Bondarev, A.V.Bragin, D.V.Chernyak, A.S.Dvoretsky, S.I.Eidelman, G.V.Fedotovich, N.I.Gabyshev, A.A.Grebeniuk, D.N.Grigoriev, P.M.Ivanov, S.V.Karpov, V.F.Kazanin, B.I.Khazin, I.A.Koop, P.P.Krokovny, L.M.Kurdadze, A.S.Kuzmin, I.B.Logashenko, P.A.Lukin, A.P.Lysenko, K.Yu.Mikhailov, I.N.Nesterenko, V.S.Okhapkin, E.A.Perevedentsev, E.A.Panich, A.S.Popov, T.A.Purlatz, N.I.Root, A.A.Ruban, N.M.Ryskulov, A.G.Shamov, Yu.M.Shatunov, B.A.Shwartz, A.L.Sibidanov, V.A.Sidorov, A.N.Skrinsky, V.P.Smakhtin, I.G.Snopkov, E.P.Solodov, P.Yu.Stepanov, A.I.Sukhanov, V.M.Titov, Yu.V.Yudin, S.G.Zverev

Study of the ϕ decays into $\pi^+\pi^-\gamma$, $\pi^0\pi^0\gamma$ and $\eta\pi^0\gamma$ final states

П.П. Ахметшин, Е.В. Анашкин и др.
(всего 53 авторов)

Изучение распадов ϕ мезона в $\pi^+\pi^-\gamma$, $\pi^0\pi^0\gamma$ и $\eta\pi^0\gamma$ конечные состояния

Budker INP 99-51

Ответственный за выпуск А.М. Кудрявцев
Работа поступила 8.06.1999 г.

Сдано в набор 15.06.1999 г.
Подписано в печать 15.06.1999 г.
Формат бумаги 60×90 1/16 Объем 1.9 печ.л., 1.6 уч.-изд.л.
Тираж 150 экз. Бесплатно. Заказ N° 51

Обработано на IBM PC и отпечатано на
ротапринте ИЯФ им. Г.И. Будкера СО РАН
Новосибирск, 630090, пр. академика Лаврентьева, 11.